International Journal of Pharmaceutics 493 (2015) 224–232

Contents lists available at ScienceDirect

International Journal of Pharmaceutics

journal homepage: www.elsevier.com/locate/ijpharm

Formulation and nebulization of fluticasone propionate-loaded lipid nanocarriers

Anita Umerska[a,*], Celia R.A. Mouzouvi[a,b], André Bigot[c], Patrick Saulnier[a]

[a] INSERM U1066, University of Angers, France
[b] Laboratoire de Pharmacie Galenique, UFR Pharmacie, FSS, Université d'Abomey-calavi, Cotonou, Benin
[c] Unité d'Immunologie, Faculté des Sciences de la Santé, Université d'Abomey-calavi, Cotonou, Benin

ARTICLE INFO

Article history:
Received 2 May 2015
Received in revised form 1 July 2015
Accepted 2 July 2015
Available online 14 July 2015

Keywords
Lipid
Nanocarriers
Fluticasone propionate
Nebulization
Drug delivery system
Aerosol
Inhalation

ABSTRACT

Inhaled fluticasone propionate (FP) is often prescribed as a first-line therapy for the effective management of pulmonary diseases such as asthma. As nanocarriers offer many advantages over other drug delivery systems, this study investigated the suitability of lipid nanocapsules (LNCs) as a carrier for fluticasone propionate, examining the drug-related factors that should be considered in the formulation design and the behaviour of LNCs with different compositions and properties suspended within aerosol droplets under the relatively hostile conditions of nebulization.

By adjusting the formulation conditions, particularly the nanocarrier composition, FP was efficiently encapsulated within the LNCs with a yield of up to 97%, and a concentration comparable to commercially available preparations was achieved. Moreover, testing the solubility of the drug in oil and water and determining the oil/water partition coefficient proved to be useful when assessing the encapsulation of the FP in the LNC formulation.

Nebulization did not cause the FP to leak from the formulation, and no phase separation was observed after nebulization. LNCs with a diameter of 100 nm containing a smaller amount of surfactant and a larger amount of oil provided a better FP-loading capacity and better stability during nebulization than 30 or 60 nm LNCs.

© 2015 Elsevier B.V. All rights reserved.

1. Introduction

Pulmonary diseases such as asthma and chronic obstructive pulmonary disease (COPD) affect millions of people worldwide. Inhalation is the preferred route of drug administration for asthma treatment (Borgström, 2001). Pulmonary administration offers many advantages for the treatment of respiratory diseases compared with other routes of delivery. Inhalation therapy allows for the direct application of a drug within the lungs (Beck-Broichsitter et al., 2009). Direct delivery of the active substances to the lung enables the administration of lower doses compared with other routes of administration (i.e., oral, buccal, or rectal delivery) with an equivalent therapeutic response and lower systemic exposure (Arzhavitina and Steckel, 2010). Inhaler devices are commonly used for the local delivery of drug molecules to treat pulmonaty diseases such as COPD and asthma. Four broad classes of inhalation devices are used to administer these drugs, including pressurized metered dose inhalers, nebulizers, soft mist inhalers, and dry powder inhalers (Cipolla et al., 2014). Nebulizers are recommended for children and adults have difficulty coordinating inspiration and aerosol actuation and in acute severe episodes of bronchospasms. Nebulization can also be indicated when a patient requires large doses of inhaled drugs (Arzhavitina and Steckel, 2010).

Inhaled glucocorticosteroids are often prescribed as the first-line therapy for the effective management of persistent asthma (Dahl, 2006). The most commonly prescribed inhaled corticosteroid is fluticasone propionate (FP), a highly potent anti-inflammatory drug with good pharmacokinetic and pharmacodynamic properties (Chiang et al., 2010). Compared with other inhaled corticosteroids (triamcinolone acetonide, flunisolide, beclomethasone dipropionate, and budesonide), FP has the highest affinity to the corticosteroid receptor relative to dexamethasone (RRA = 1800) and the lowest systemic bioavailability (<1%). Reports have indicated that 80% of FP is bound to plasma proteins (Derendorf et al., 1998).

Drug absorption and retention in the lungs is dependent on many factors such as the physico-chemical properties of the drug,

* Corresponding author at: INSERM U1066, IBS-IRIS Niveau 3, Rue des Capucins, 49933 Angers Cedex 9, France.
E-mail address: anitaumerska@yahoo.fr (A. Umerska).

http://dx.doi.org/10.1016/j.ijpharm.2015.07.008
0378-5173/© 2015 Elsevier B.V. All rights reserved.

the formulation and the method of delivery (Yang et al., 2008). Fluticasone for inhalation is available as a dry powder inhaler, an inhalation aerosol (a suspension of FP with suitable propellants in a pressurized container) and a micronized suspension for nebulization.

Recently, the use of nanoparticles for drug delivery has received a great deal of attention from researchers due to their efficacy and safety, and the advantages offered by nanoparticles are widely accepted by industry (Chiang et al., 2010). Nanoparticles offer numerous advantages over other delivery systems due to their special characteristics including their small particle size and large surface area and the ability to control their surface properties (Azarmi et al., 2008). Drug encapsulation within nanocarriers protects the encapsulated molecules from direct biological interactions, protects them from degradation, and reduces their potential systemic toxicity. Encapsulation can also improve the therapeutic efficiency by controlling the biodistribution and release kinetics of the active pharmaceutical ingredient (API; Delmas et al., 2012). Nanoscale suspensions offer several advantages compared with solutions and dry powder formulations including their suitability for poorly soluble crystalline compounds (therefore eliminating the need for solubilization), the ease of dosing with a syringe-type delivery device in animal studies (leading to more consistent drug distribution in the lung compared with dry powder formulations), and the ability to control the particle size (reducing the variability in drug absorption) (Yang et al., 2008).

The fate of inhaled nanomaterials depends on regional distribution in the lung (Sakagami, 2006). The inertial impaction and sedimentation occur during the passage through the oropharyngeal region or the bronchial region, respectively, and it affects particles larger than 10 μm in diameter. At the other extreme, particles smaller than 1 μm are likely to reach the alveolar region, but they are expected to be exhaled rather than deposited. Particles with aerodynamic diameters between 1 and 5 μm are likely to be deposited in the lung periphery (Bailey and Berkland, 2009). Individual nanoparticles are too small to be deposited in the alveoli and the majority of the administered dose is exhaled. The nanoparticles are most often delivered to the lungs via nebulization of colloidal suspensions (Sung et al., 2007), and in this case it is the size of the aqueous droplet that determines the fate of the inhaled nanocarriers. To administer the nanoparticles in the solid state form, Trojan particles (nanoparticles incorporated into microparticles) can be employed (Tsapis et al., 2002).

Lipids have been widely used in a variety of drug delivery systems such as liposomes, emulsions, solid lipid nanoparticles (SLNs) and nanostructured lipid carriers (NLCs). These formulations were not developed specifically for pulmonary applications, but they have since been used for respiratory delivery as scientists have explored novel applications in various pharmaceutical areas (Cipolla et al., 2014). A number of pharmaceutical liposome formulations have reached the market, and many liposome formulations have shown promise as inhaled products (Cipolla et al., 2014). In contrast, the evaluation of the potential of SLNs and NLCs to provide therapeutic benefit as inhaled products is at an earlier stage (Weber et al., 2014). Lipid nanocarriers can be used to solubilize poorly water-soluble drugs. One major advantage of these systems is that their solubilization capacity is retained on administration, in contrast to formulations based on conventional solubilization approaches. Formulations containing cosolvents or surfactant micelles may partially lose their solubilization potential upon dilution with aqueous media (Bunjes, 2010).

A broad range of drugs, mainly drugs with lipophilic properties, has already been incorporated into lipid nanocapsules (LNCs), including ibuprofen (Lamprecht et al., 2004), etoposide (Lamprecht and Benoit, 2006), paclitaxel (Hureaux et al., 2009), and amiodarone (Lamprecht et al., 2002). LNCs can be considered as drug carriers for various routes of administration, including oral and local delivery (Huynh et al., 2009). Recently, researchers have investigated pulmonary administration of LNCs (Hureaux et al., 2009). Hureaux et al. (2009) examined the nebulization of drug-free and paclitaxel-loaded LNCs. That study focused on the selection of the nebulizer device and the properties of the resulting aerosol. However, the influence of nanoparticle characteristics and concentration were not investigated, with only 50 nm LNCs tested at one concentration. The characteristics of nanoparticles and liposomes including their composition have been shown to exert an important influence on their stability and possible aggregation upon nebulization (Dailey et al., 2003; Kleemann et al., 2007). Indeed, the performance of liposomes during nebulization strongly depended on the composition of the lipids and the drug, with characteristics such as particle size and surface charge exhibiting significant effects (Niven and Schreier, 1990; Niven et al., 1991; Desai et al., 2002). As the size and composition of LNCs can vary (Heurtault et al., 2002; Lamprecht et al., 2002; Huynh et al., 2009), it is important to examine the influence of these factors on the behaviour of nanocarriers during nebulization.

The objective of this study was to investigate the suitability of LNCs as carriers for fluticasone propionate and to determine which drug factors should be considered in the formulation design. Another important goal of this work was to examine the behaviour of the different LNCs suspended within aerosol droplets under the relatively aggressive conditions of nebulization.

2. Materials and methods

2.1. Materials

Labrafac® CC (caprylic/capric acid triglycerides-C8/C10-TG) was kindly provided by Gattefossé S.A. (France). Lipoid® S75-3 (hydrogenated lecithin) and Solutol® HS15 (macrogol 15 hydroxystearate, polyoxyl 15 hydroxystearate) were kindly provided by Lipoid Gmbh (Germany) and BASF (Germany), respectively. Fluticasone propionate was purchased from Kemprotec (UK). All other chemicals and solvents were of analytical grade. Amicon Ultra-4 centrifugal filter devices were obtained from Millipore (USA).

2.2. Solubility in oil and in water

In a glass scintillation vial, 50 mg of FP and 10 ml of C8/C10-TG, water or a 0.5% (w/v) aqueous solution of polyoxyl 15 hydroxystearate were heated up to 95–100 °C for 5 min. Samples were cooled down to room temperature and centrifuged (16,000 × g, 5 min) to remove undissolved FP, and the supernatant was diluted with acetonitrile (1:20 and 1:1 volume ratios for the C8/C10-TG and aqueous solutions, respectively). The solubility of FP was determined by measuring the absorbance at an operating wavelength of 250 nm in optically homogenous quartz cuvettes (Hellma) with a light path of 10 mm, with mixtures of C8/C10-TG/acetonitrile, water/acetonitrile, and polyoxyl 15 hydroxystearate solution/acetonitrile used as references. The absorbance measurements were performed using a UV-2600 spectrophotometer (Shimadzu).

2.3. Thermal stability of FP

1 mg of FP dissolved in 10 ml of C8/C10-TG was heated up to 95–100 °C and then cooled to 60 °C; this cycle was repeated three times, and after the final cycle the dispersion was cooled down to room temperature. Then, 0.2 ml of the solution of FP in C8/C10-TG was mixed with 1.8 ml of acetonitrile (1:10 v/v dilution, 10 μg of FP/ml). As a control, FP was dissolved in acetonitrile and mixed with C8/C10-TG without heating. Due to the high absorbance of the

Table 1
Composition of lipid nanocarriers.

	LNC30 (%)	LNC60 (%)	LNC100 (%)
Polyoxyl 15 hydroxystearate	67.76	43.41	27.38
Hydrogenated lecithin	2.60	3.85	4.24
C8/C10-TG	29.64	52.74	68.38

samples at lower wavelengths (190–250 nm), it was necessary to further dilute (1:200, v/v dilution, 0.5 μg of FP/ml) the samples in acetonitrile.

Samples and the reference (acetonitrile) were placed in optically homogenous quartz cuvettes (Hellma) with a 10 mm light path. The UV spectra of the solutions were recorded at wavelengths between 190 and 400 nm using a UV-2600 spectrophotometer (Shimadzu).

2.4. Lipophilic/hydrophilic drug properties

To examine the partition of FP between water and C8/C10-TG, FP was dissolved in C8/C10-TG at 0.25 mg/ml and mixed with water at a 1:1 (v/v) ratio. The mixture was magnetically stirred (900 rpm) and heated to 95 °C and then cooled to 60 °C; this cycle was repeated three times, and after the final cycle the dispersion was cooled to room temperature. The bottom phase (water) remained transparent, while the upper phase (C8/C10-TG) became turbid. As a control, the mixture of water and C8/C10-TG (1:1, v/v ratio) was also exposed to the same heating/cooling cycles, and the upper oil phase also became turbid in the control sample. Then, 1 ml of the bottom aqueous phase was diluted with 1 ml of acetonitrile and 0.2 ml of the upper phase (C8/C10-TG) was diluted with 1.8 ml of acetonitrile. After dilution with acetonitrile, the C8/C10-TG dispersion became transparent. The absorbance at an operating wavelength of 250 nm was recorded as described in Section 2.2.

2.5. Preparation of LNCs

LNCs were prepared following the procedure described by Heurtault et al. (2002) at a concentration of 177 mg/ml, with the composition of each formulation presented in Table 1. The components of the LNCs (polyoxyl 15 hydroxystearate, hydrogenated lecithin, and C8/C10-TG) and NaCl (0.089 g) were weighed, mixed with 1.1 or 3.1 ml of water (LNC30 and LNC60, LNC100, respectively) and heated to 95–100 °C. Optionally, 0.125, 0.25, or 0.5 ml of FP dissolved in acetone at 20 mg/ml was added. The samples were cooled to 60 °C. The samples were treated with three heating-cooling cycles, and during the last cooling cycle, at 80–90 °C (the temperature of the phase inversion) the system was diluted with cold (~4 °C) water up to a final volume of 10 ml. Formulations were left overnight to allow acetone to evaporate, and additional water was added to return the final volume to 10 ml if necessary.

2.6. Selection of a wavelength for FP quantification and preparation of calibration curves

The spectra of an FP solution (0.06 mg/ml) in acetonitrile or in a mixture of acetonitrile and water (1:1 and 5:1) were recorded at wavelengths between 190 and 400 nm. To prepare calibration curves, FP was dissolved in acetonitrile or in the mixture of acetonitrile and water (1:1 and 5:1 ACN to W volume ratios). The absorbances of FP solutions at concentrations between 1 and 500 μg/ml were measured using appropriate solvent mixtures as references. To prepare the calibration curves, the absorbance of FP solutions at concentrations between 0.1 and 500 μg/ml in acetonitrile or in water/acetonitrile mixtures were measured at 250 nm. The calibration curves obtained for different water/acetonitrile ratios were found to be linear for FP concentrations between 0.5 and 125 μg/ml.

2.7. Separation of FP from the nanocarriers and quantification of FP

FP was separated from the LNC suspension by centrifugation (4500 × g, 10 min). The sediment (non-encapsulated FP) was washed twice with water, dried, and dissolved in acetonitrile. The supernatant containing FP-loaded LNCs and dissolved non-encapsulated FP was subjected to a combined ultrafiltration-centrifugation technique using Amicon Ultra-4 centrifugal filter devices with a molecular weight cut off (MWCO) of 10 kDa. Then, 2 ml of drug loaded LNCs (or unloaded control LNCs) were added to the filter device and centrifuged for 2 h (4500 × g). Then, deionized water was added to the sample remaining in the filter device (containing encapsulated FP) to a volume of 2 ml. Of this volume, 0.4 ml was then transferred into a 2 ml Eppendorf tube and diluted with 1.6 ml acetonitrile to break up the particles and extract the encapsulated FP, and then centrifuged (16,000 × g) for 30 min to remove aggregated particles. The absorbance of the supernatant was then measured at 250 nm with a 1:5 water:acetonitrile mixture as a reference. The filtrate containing non-encapsulated FP, collected from the bottom of the centrifuge tube, was diluted with acetonitrile at a 1:1 volume ratio, and its absorbance was measured at an operating wavelength of 250 nm as described in Section 2.2, using a 1:1 acetonitrile:water mixture as a reference. LNC formulations without FP were also subjected to the same procedures. Their absorbance was treated as a blank and was subtracted from the reading of FP-loaded formulations.

The encapsulation efficiency (EE) and drug loading (DL) were calculated using the following equations:

$$EE = \frac{B}{A} * 100\% \quad (1)$$

where A is the total amount (mass) of the FP, and B is the mass of the encapsulated FP;

$$DL = \frac{B}{C} * 100\% \quad (2)$$

where C is the total weight of all components of the LNCs.

2.8. Characterization of LNCs

The intensity-averaged particle diameter and the polydispersity indexes of the LNCs were determined by Dynamic Light Scattering (DLS) with 173° backscatter detection. The electrophoretic mobility values measured by Laser Doppler Velocimetry (LDV) were converted to zeta potential by the Smoluchowski equation. Both DLS and LDV measurements were carried out on a Zetasizer nano series Nano-ZS fitted with a 633 nm laser (Malvern Instruments, UK). The measurements were performed at an LNC concentration of 3 mg/ml, obtained after dilution with MilliQ water. Each analysis was carried out at 25 °C in triplicate.

To obtain the size distribution by intensity, volume and number, data were processed using the Zetasizer software (version 7.02), and the multiple narrow modes (high resolution) model was applied.

2.9. Nebulization of LNCs

The e-Flow® rapid vibrating mesh nebulizer was used to nebulize 3 ml of LNC dispersions. LNCs without FP were nebulized at three concentrations: 177, 17.7, and 3.54 mg/ml, while FP-loaded formulations were nebulized only at the highest concentrations

Table 2
Solubility of FP in different solvents, approximate weight of solvent necessary to dissolve 1 g of FP (the density values used for calculation were: 1000 g/L for water and aqueous solution of polyoxyl 15 hydroxystearate, and 945 g/L for C8/C10-TG).

Solvent	Solubility of FP	Approximate weight of solvent (g) necessary to dissolve 1 g of FP	Description of solubility according to European Pharmacopoeia or USP
C8/C10-TG	2.25 ± 0.04 mg/g	420	Slightly soluble
0.5% w/v aqueous solution of polyoxyl 15 hydroxystearate	62 ± 13 μg/g	16,129	Practically insoluble
Water	0.7 ± 0.3 μg/g	1,428,571	Practically insoluble

(177 and 17.7 mg/ml). Formulations were diluted with 0.9% (w/v) NaCl aqueous solution.

The volume of the sample remaining in the nebulizer after nebulization was measured each time and was found to be approximately 1 ml. The nebulization time was also measured. To calculate the nebulizer output, the nebulization time was divided by the amount of the formulation nebulized (2 ml).

FP was extracted from LNCs and quantified (see Section 2.7) before and after nebulization.

2.10. Statistical analysis

The statistical significance of the differences between samples was determined using one-way analysis of variance (ANOVA). Differences were considered significant at $p < 0.05$.

3. Results and discussion

3.1. Selection of a wavelength for FP quantification

To investigate the possibility of interference from other formulation components, the spectra of FP and the LNCs without FP were recorded. The results show that the spectra of FP in mixtures of water (W) and acetonitrile (ACN) at different volume ratios are similar (Fig. 1). The highest absorbance of UV radiation by FP was observed at approximately 240 nm, and the maximum was slightly shifted towards higher wavelengths as the W/ACN (water/acetonitrile) ratio increased (a bathochromic shift). However, the spectra of supernatants from disrupted LNCs demonstrate that other components of the formulation also exhibited a significant absorbance at 240 nm. Therefore, 250 nm was selected as the wavelength for FP quantification.

3.2. Drug factors to be considered in formulation design

Each dosage form requires careful study of the physical and chemical properties of active ingredients to achieve a stable, efficacious product. Previous studies of LNCs (Heurtault et al., 2002; Huynh et al., 2009; Hirsjarvi et al., 2012) suggest that the following properties may be important: drug solubility, partition coefficient, and thermal stability.

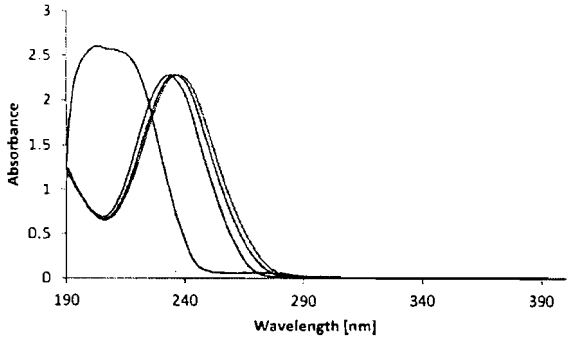

Fig. 1. UV spectra of FP solutions in acetonitrile (violet), water/acetonitrile 1/5 (v/v) (green), water/acetonitrile 1/1 (v/v) (red) and the supernatant from the LNC100 preparation in acetonitrile 1/5 (v/v) (blue). (For interpretation of the references to color in this figure legend, the reader is referred to the web version of this article.)

The solubilities of FP in water, an aqueous solution of polyoxyl 15 hydroxystearate and C8/C10-TG are reported in Table 2. FP is practically insoluble in water, in good agreement with its pharmacopeial monograph. While the addition of polyoxyl 15 hydroxystearate led to a 90-fold increase in the solubility of FP 90, according to the pharmacopeial definition FP remained practically insoluble.

Solutol® HS15 (polyoxyl 15 hydroxystearate) consists of polyglycol mono- and di-esters of 12-hydroxystearic acid and approximately 30% free polyethylene glycol. Solutol® is a non-ionic solubilizer and an o/w emulsifying agent with an HLB value between 14 and 16. Solutol is soluble in water, but its solubility decreases with increasing temperature (manufacturer's data). Polyoxyethylene-type non-ionic surfactants become more lipophilic as temperature increased due to the dehydration of polyoxyethylene chains resulting from the breakdown of hydrogen bonds with water molecules (Huynh et al., 2009). Solubility studies (Section 2.2) demonstrated that the cloud point (the temperature at which the surfactant is no longer completely soluble) of polyoxyl 15 hydroxystearate was approximately 63 °C.

FP was slightly soluble in C8/C10-TG. This is in agreement with the data obtained by Doktorová et al. (2010) that the solubility of FP in a wide array of solid and liquid lipids was below 0.3% despite the high lipophilicity of FP. Poorly water-soluble drugs do not necessarily display high lipid solubility. When strong intermolecular binding forces resulting in a high crystal lattice energy are present, drug substances usually have a high melting point and are often not very soluble in either water or oil. Indeed, drugs successfully formulated in emulsions are often characterized by a rather low melting temperature (Bunjes, 2010). The high melting point of FP (272–273 °C) may explain its relatively low solubility in C8/C10-TG.

Apart from its solubility in oil, partitioning of the drug between the oil and aqueous phases has to be considered during LNC formulation design. The log *P* value defines the ratio at which a drug will dissolve in each phase of an oil-water system, and thus represents a measure of the hydrophobicity of the drug. After mixing C8/C10-TG with water, the upper oil-rich phase became turbid in both the FP sample and the control (C8/C10-TG and water without FP). In the FP sample, 97.7 ± 2.3% was detected in the oil phase and only 0.6 ± 0.25% was present in the aqueous phase (Table 3). This distribution of FP between the aqueous and oil phases is in agreement with the solubility data. The concentration of FP in the oil phase is approximately 163 times higher than that in water, and the logarithm of the ratio of the concentrations in the solvents, log *P*, is 2.2.

One of the most important aspects of LNC formulations is the chemical stability of the drug. During formulation in LNCs, the drug

Table 3
Partitioning of FP between water and oil (C8/C10-TG).

Phase	FP conc [μg/ml]	% of the total amount of FP
Oil	244 ± 6	97.7 ± 2.3
Water	1.5 ± 0.6	0.6 ± 0.25

may be exposed to high temperatures up to 100 °C. As FP does not dissolve in water or in a water–oil mixture and it is mainly present in the oil phase, the stability studies were performed in C8/C10-TG. The UV spectra of FP dissolved in C8/C10-TG before and after heating were superimposable (not shown), indicating that the chemical integrity of FP was maintained. As the conditions of LNC preparation do not induce degradation or structural changes in FP molecules, this drug can be safely encapsulated within LNCs.

3.3. Encapsulation of fluticasone propionate in LNCs

Small, homogenously dispersed LNCs (PDI < 0.01) were successfully obtained (Table 4). The particle diameter was strongly dependent on the proportions of the LNC components as previously reported (Heurtault et al., 2002, Huynh et al., 2009; Hirsjarvi et al., 2012). The amount of the hydrophilic surfactant (polyoxyl 15 hydroxystearate) in the LNCs was the main factor influencing the particle size (Heurtault et al., 2002). Varying the mass ratio of the LNC components (polyoxyl 15 hydroxystearate and C8/C10-TG) yielded particles with sizes ranging between 30 and 100 nm. Formulations with diameters of 30, 60, and 100 nm are named LNC30, LNC60, and LNC100, respectively, and the PDI values of these formulations did not differ significantly. All formulations were characterized by slightly negative zeta potential values between −3.5 and −10.6 mV. LNC100 exhibited a more negative zeta potential than LNC30 ($p = 0.0166$). The negative zeta potential values may be attributed to hydrogenated lecithin, as soy lecithin dispersions in NaCl solutions have been shown to bear negative zeta potentials (Manconi et al., 2003).

The incorporation of FP in LNCs did not change the LNC characteristics. The particle size, polydispersity index and zeta potential of the FP-loaded LNCs were the same as those of drug-free LNCs with the same composition. This may indicate that the drug is uniformly distributed within the core of the LNCs and that there is no significant drug adsorption on the particle surface. The lack of an influence of drug encapsulation on the LNC properties might also be due to the relatively low drug content in the particles (0.05–0.2%). Similar results were obtained by Lamprecht and Benoit (2006) for etoposide-loaded LNCs, where the incorporation of the API did not change either the particle size or the zeta potential of the LNCs (the drug loading for these LNCs was between 0.06% and 0.09%). Comparably, the encapsulation of nile red in lipid nanoparticles (drug loading 0.01–0.1%) did not significantly affect either the surface charge or the size of the carriers (Delmas et al., 2012). In contrast, the encapsulation of ibuprofen significantly affected both the size and zeta potential of the LNCs, leading to a decrease in particle size and an increase in zeta potential. The ibuprofen content in the oil phase was markedly high in these LNCs (20, 100 or 200 mg were dissolved in 993, 913 or 813 mg of C8/C10-TG, respectively) (Lamprecht et al., 2004). The encapsulation of amiodarone in LNCs did not change either the diameter or the size distribution of the LNCs, although a change in zeta potential was observed (20 mg of amiodarone were dissolved in 0.85–1.23 g of C8/C10-TG) (Lamprecht et al., 2002). Malzert-Fréon et al. (2010) examined the encapsulation of tripentone in LNCs containing the solubility enhancer with the commercial name Labrasol®. At drug-loading levels below 0.5%, the tripentone-loaded LNCs were similar in size to empty LNCs, and drug loading levels between 0.5% and 6.5% significantly increased the particle size, with a linear relationship observed between drug loading and particle size.

The FP-loaded LNCs are the smallest FP carriers described thus far. The nanoparticles produced by Doktorová et al. (2010) were significantly larger, with sizes between 316 and 408 nm. Nirale et al. (2009) described 700–800 nm liposomes with a PDI of 0.1–0.3 as carriers for FP. These liposomes also exhibited higher polydispersity index values (0.45–0.9). Yang et al. (2008) used a wet milling method with glass beads to formulate nanosuspensions of fluticasone and budesonide with a particle size (D90) of 0.4 μm. Chiang et al. (2009, 2010) produced a nanosuspension of fluticasone using a bench scale wet milling (micronization) device with glass beads; the size of the bulk material was reduced from a D50 of 35 to 0.24 μm.

As a satisfactory mass balance was obtained between the encapsulated and non-encapsulated fractions in all cases (100 ± 10%), only the encapsulated % of FP is presented in Table 4. The non-encapsulated fraction constitutes the remainder. The concentration of FP dissolved in the aqueous phase ranged between 1% and 4% of the total amount of FP. The remaining non-encapsulated FP, which comprises most of the non-encapsulated fraction, precipitated and was separated from the LNCs by sedimentation. Among FP-loaded formulations, sediment was observed in all cases with the exception of LNC100FP250. In contrast to polyelectrolyte complex nanoparticles described previously (Umerska et al., 2014a,b, 2015), the excessive amount of the API did not lead to destabilization or change the properties of the LNCs.

The encapsulation efficiency depended on the composition of the nanocarriers and the initial FP concentration. The formulation process was optimized to obtain LNCs with high encapsulation efficiency values up to 97%. High entrapment efficiency (96–97% and 95–98%) was also achieved for nanostructured lipid carriers and liposomes by Doktorová et al. (2010) and Nirale et al. (2009), respectively. The final FP concentration and the drug loading mainly depended on the composition of the formulation. In contrast to encapsulation efficiency, the drug loading did not depend on the initial amount of FP used. The FP concentrations in the LNC30, LNC60, and LNC100 formulations were approximately 0.1, 0.18, and 0.24 mg/ml. The concentration of FP in the LNC100 formulation was similar to the concentration in the manufactured product, Flixotide Nebules (0.5 mg/2 ml), indicating that this level of API encapsulation in the LNCs can be considered satisfactory despite low drug loading. LNC30, LNC60, and LNC100 formulations contain different quantities of C8/C10-TG, indicating that each LNC

Table 4
Physical properties and FP encapsulation in LNCs (EE, encapsulation efficiency; DL, drug loading; PS, particle size; PDI, polydispersity index; ZP, zeta potential).

	EE	DL	Final conc. of FP	PS	PDI	ZP
LNC30	0	0	0	30.2 ± 1.5	0.081 ± 0.026	−4.98 ± 1.57
LNC30FP250	38.6 ± 5.0	0.055 ± 0.007	0.097 ± 0.013	28.4 ± 0.3	0.060 ± 0.014	−4.10 ± 0.29
LNC30FP500	20.8 ± 2.0	0.059 ± 0.006	0.104 ± 0.010	28.2 ± 0.2	0.070 ± 0.028	−3.47 ± 0.58
LNC30FP1000	11.1 ± 2.3	0.063 ± 0.013	0.111 ± 0.023	28.9 ± 0.8	0.076 ± 0.014	−4.35 ± 0.76
LNC60	0	0	0	58.1 ± 0.3	0.038 ± 0.009	−8.61 ± 2.51
LNC60FP250	72.6 ± 7.4	0.103 ± 0.011	0.182 ± 0.019	58.5 ± 2.1	0.035 ± 0.009	−7.32 ± 1.02
LNC60FP500	36.4 ± 4.6	0.103 ± 0.014	0.182 ± 0.023	58.2 ± 1.1	0.045 ± 0.011	−6.78 ± 1.20
LNC60FP1000	17.8 ± 2.7	0.101 ± 0.015	0.178 ± 0.027	58.4 ± 1.0	0.045 ± 0.011	−9.07 ± 2.10
LNC100	0	0	0	99.6 ± 2.2	0.047 ± 0.013	−10.62 ± 1.90
LNC100FP250	97.1 ± 2.4	0.138 ± 0.003	0.243 ± 0.006	102.5 ± 1.5	0.050 ± 0.014	−8.50 ± 0.93
LNC100FP500	50.5 ± 4.6	0.142 ± 0.013	0.252 ± 0.023	103.2 ± 0.7	0.060 ± 0.014	−8.38 ± 0.92
LNC100FP1000	23.8 ± 6.8	0.134 ± 0.039	0.238 ± 0.068	102.5 ± 3.4	0.054 ± 0.026	−8.91 ± 1.75

formulation is capable of encapsulating a certain quantity of FP depending on the quantity of oil in the formulation. Therefore, the LNC100 formulation has a better encapsulation efficiency than the LNC60 and LNC30 formulations. Samples with higher initial FP concentrations had lower EEs. FP was slightly soluble in C8/C10-TG and practically insoluble in other components of the formulation. Therefore, when the amount of FP exceeded the maximum amount that could be dissolved in C8/C10-TG, the excess FP precipitated. After FP encapsulation, the FP concentration in the C8/C10-TG in the oil phase of the formulations was close to 0.2% (i.e., 2 mg of FP/g of oil), in good agreement with the solubility data. This loading is higher than that in the nanostructured lipid carriers described by Doktorová et al. (2010), who obtained 0.1% loading of FP in the lipid phase. The saturation concentration of many drug molecules (including for hydrophobic drugs) in lipids is known to be relatively low (below 1%) and is further reduced in crystalline lipids (Cipolla et al., 2014). For instance, nile red was found to crystallize at concentrations above 0.1% in all tested lipid mixtures, and its maximal loading in lipid nanoparticles was found to be approximately 0.1% (Delmas et al., 2012). Lipid nanoparticles and other lipophilic carriers are generally characterized by lower drug loading (0.5–5%) compared with hydrophilic carriers intended for the encapsulation of hydrophilic compounds, where drug loading values up to 50% can be achieved with optimized formulation processes (Umerska et al., 2014a,b).

Lamprecht et al. (2002) examined the influence of particle size (and consequently the composition) on the encapsulation of amiodarone in LNCs. The encapsulation efficiency values obtained were highly similar across LNCs in this study, ranging from 92.1 ± 1.3% to 93.0 ± 2.5%. This may be due to the different experimental design in this study, in which amiodarone was dissolved prior to the formulation of the LNCs, with the result that amiodarone was sufficiently soluble in the oil phase and the limiting dose was not achieved. The high EE values were attributed to the 'nearly negligible' solubility of amiodarone in water. Similarly, high encapsulation efficiencies in LNCs were obtained for ibuprofen (Lamprecht et al., 2004) due to its low solubility in the external aqueous phase. Tripentone-loaded LNCs were also characterized by a high EE (Malzert-Fréon et al., 2010). High encapsulation efficiencies (between 86.4% and 93.4%) were also observed in etoposide-loaded LNCs (Lamprecht and Benoit, 2006), with 25 nm LNCs characterized by a lower EE than 100 nm LNCs (86.4 ± 3.2% and 93.4 ± 2.5% for 25 nm and 100 nm LNCs, respectively). The drug loading in this study (0.058–0.091%) was comparable to our results. In conclusion, the encapsulation of lipophilic compounds in LNCs depends on the solubility of the drug in the oil phase. A high encapsulation efficiency can be obtained if this solubility is not exceeded, with the solubility of the drug in water and the lipid/water partition coefficient also exerting effects. If the quantity of the lipophilic drug in the LNCs is higher than the solubility of the drug in the oil phase, the drug precipitates and phase separation can be observed. The precipitated drug does not influence the properties of the carrier and can be separated by sedimentation. If the solubility of the drug in oil is limited, then formulations containing higher oil/surfactant mass mixing ratios are preferred as they have better loading capacities. Moreover, examining the solubility of the drug in oil and water as well as the oil/water partition coefficient is useful in assessing the drug encapsulation in the LNC formulation.

3.4. Nebulization of the LNCs

The vibrating mesh nebulizer offered important advantages over air-jet and ultrasonic nebulizers for the nebulization of liposomal formulations of iloprost, including high output, protecting the stability of nebulized liposomes, and the production of small aerosol droplets (Kleemann et al., 2007). The vibrating mesh nebulizer was selected for the nebulization studies here, as it has previously been shown to perform better than jet or ultrasonic nebulizers (Hureaux et al., 2009).

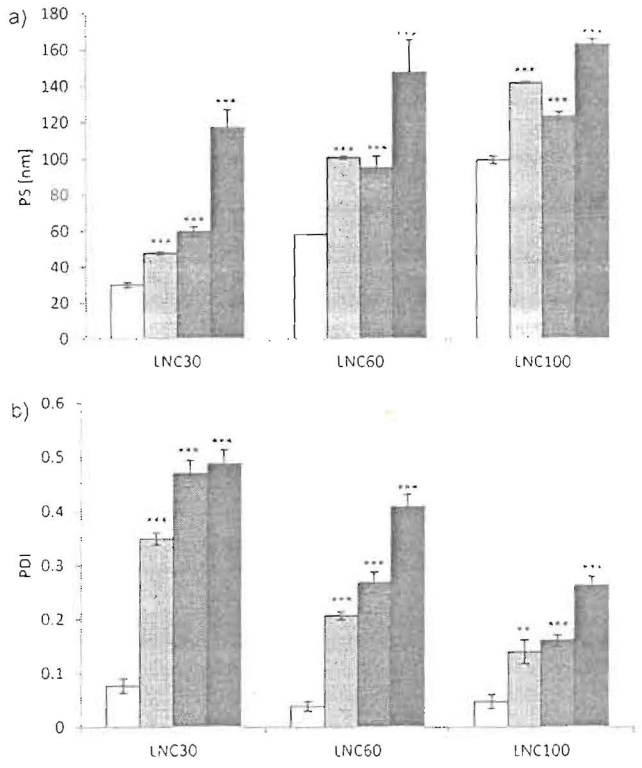

Fig. 2. The properties of LNCs before nebulization (white bars) and after nebulization at 17.7 mg/ml (light grey bars), 17.7 mg/ml (dark grey bars) and 3.54 mg/ml (black bars); (a) particle size and (b) polydispersity index. $^{*}p < 0.05$, $^{**}p < 0.01$, and $^{***}p < 0.001$ versus drug-free LNCs (white bars).

Neither phase separation nor macroscopic aggregation was observed after the nebulization of the LNC formulations. The zeta potential of the LNCs was the same before and after nebulization (not shown). DLS measurements revealed that the particle size and polydispersity index increased significantly after nebulization (Fig. 2). Surprisingly, the increase in particle size was greater in less concentrated formulations for all LNC compositions tested here. LNC30 were more markedly affected by the nebulization than the other LNCs. The particle size of this formulation increased fourfold after nebulization at a concentration of 3.5 mg/ml, and the size doubled after nebulization at 17.7 mg/ml (Fig. 2a). LNC60 doubled in size after nebulization at concentrations of 17.7 and 177 mg/ml, and increased threefold in size after nebulization at 3.5 mg/ml. The physico-chemical characteristics of LNC100 were best preserved, increasing 40%, 20%, and 60% after nebulization at concentrations of 177, 17.7, and 3.5 mg/ml, respectively, significantly smaller than the increases observed for the other formulations.

Similarly to particle size, the largest increase in polydispersity index was observed for the LNC30 formulations (Fig. 2b). The PDI values increased from less than 0.1 to 0.32–0.51 depending on the concentration. Therefore, after nebulization this formulation can no longer be considered homogenously dispersed. The polydispersity index of LNC60 also increased after nebulization from less than 0.1 to 0.20–0.27 when nebulized at concentrations of 17.7 or 177 mg/ml, or to 0.41 when nebulized at a concentration of 3.5 mg/ml. The PDI of nebulized LNC100 also increased from less than 0.1 to 0.12–0.14, 0.16–0.17, and 0.27 when nebulized

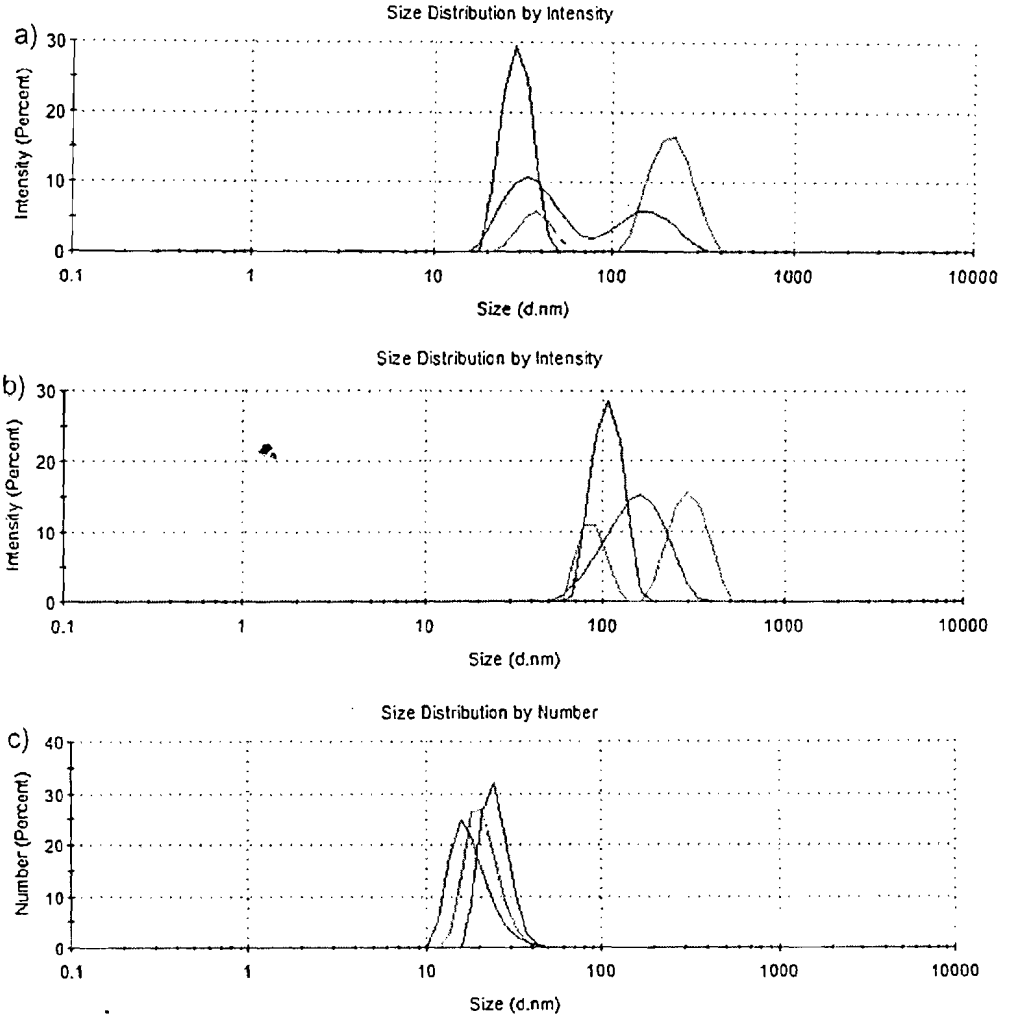

Fig. 3. Size distribution by intensity and number of drug-free LNC formulations before nebulization (black), and after nebulization at 177 mg/ml (blue), 17.7 mg/ml (green), and 3.5 mg/ml (red). Data were processed using Zetasizer software, and the multiple narrow modes (high resolution) model was applied (a) LNC100 size distribution by intensity, (b) LNC60 size distribution by intensity, (c) LNC30 size distribution by intensity, (d) LNC30 size distribution by volume, (e) LNC30 size distribution by number. (For interpretation of the references to color in this figure legend, the reader is referred to the web version of this article.)

at concentrations of 177, 17.7, and 3.5 mg/ml, respectively. These increases were markedly smaller compared with those observed for LNC30 and LNC60. The results obtained for the LNC60 formulations are in good agreement with the data presented by Hureaux et al. (2009).

As the largest increase in particle size was observed at the lowest concentration tested, FP-loaded LNCs were only nebulized at concentrations of 17.7 and 177 mg/ml. The incorporation of FP did not have any important effect on the properties of nebulized LNCs (not shown).

The intensity distribution curves of the nebulized LNCs most often exhibited a bimodal size distribution, implying that particle aggregation occurred during the nebulization process (Fig. 3). Either 2 or 3 peaks were observed in the size distribution by intensity curves for LNC30 (Fig. 3a) and LNC60 (not shown). The size distribution was bimodal after nebulization of LNC100 at 3.5 mg/ml, but when LNC100 were nebulized at higher concentrations (17.7 and 177 mg/ml) only one peak was observed, indicating that despite an increase in the PDI value, the homogenous size distribution was maintained (Fig. 3b). Therefore the intensity-averaged particle size calculated by the instrument for samples with bimodal or multimodal size distribution is not representative for the particle population. Fig. 3c shows the number distribution of the entire particle population for LNC30, the properties of which were more affected by nebulization compared with the LNC60 and LNC100 formulations. The intensity of the scattered light (I) is proportional to the diameter of the particle to the power 6 (d^6) according to the Rayleigh approximation. This d^6 factor means that the total light scattered by small particles is relatively small compared to the amount of light scattered by larger particles. A small number of larger aggregates may be responsible for the larger particle diameter peaks in the intensity distribution. Indeed, the volume and number size distribution graphs show that the size of the majority of the particles did not increase. Similar phenomena were observed by Dailey et al. (2003) for poly(lactide-co-glycolide) nanoparticles and confirmed by microscopic images. PLGA nanoparticles were also prone to aggregation, although the amount of particle aggregation remained generally low (Dailey et al., 2003). The aggregation was attributed to the possible increase in fluid concentration during jet nebulization due to solvent evaporation, the shear forces involved in the generation of the aerosol, and the specific design of the jet nebulizer system, all of which contribute to the higher frequency of particle contact. The tendency towards aggregation was particularly great for particles with

relatively hydrophobic surfaces, with less aggregation observed for nanoparticles with hydrophilic surfaces. Factors increasing the frequency of particle contact may also play a role in the increase in the LNC particle size after nebulization, although the greater increase in particle size when nebulization occurs at lower concentrations implies that other issues need to be considered as well.

In many ways, colloidal particles act in like surfactant molecules in various types of dispersions (Binks, 2002). LNCs have been shown to adsorb at the air/water interface, forming a monolayer (Heurtault et al., 2003; Minkov et al., 2005). At the air/water interface, some of the polyoxyl 15 hydroxystearate molecules are thought to be released from the particle surface, followed by the reorganization of the LNC structure. The spreading of polyoxyl 15 hydroxystearate molecules at air/water interface is slower than that of triglycerides (Heurtault et al., 2003; Minkov et al., 2005). During the nebulization process, the bulk liquid is transformed into an aerosol, which has a far greater air/water interface area compared with bulk liquid. The LNCs adsorb at the increased air/water interface until the surface is fully covered by the particles. As the polyoxyl 15 hydroxystearate molecules are released, the LNCs may fuse and aggregate. This phenomenon could be more pronounced at lower LNC concentrations, where the ratio of the amount of LNCs adsorbed at the air/water interface to the amount of LNCs remaining in the bulk of the liquid or in the water droplet is larger than at higher LNC concentrations, increasing the percentage of LNCs affected by aggregation. Lecithin stabilized the LNC structure, and nanocapsules with greater lecithin content were found to be more stable at the interface compared with the LNCs with lower lecithin quantities (Minkov et al., 2005). This is in agreement with our results on the stability after nebulization of LNC100 > LNC60 > LNC30, corresponding to a decreasing quantity of lecithin in the formulation. As the amount of lecithin is markedly smaller than polyoxyl 15 hydroxystearate or C8/C10-TG, it is likely that two populations of the LNCs exist, one without lecithin molecules and another one with tightly packed lecithin monolayer around the triglyceride core (Minkov et al., 2005). It was previously established (Minkov et al., 2005) that the LNCs without phospholipid molecules lose their mechanical stability and undergo disaggregation at air/water interface leading to the formation of a true monolayer composed of triglycerides from the core of LNCs. In the case of FP-loaded LNCs, the film at the air/water interface of microdroplets may contain some FP molecules. The importance of such effect could depend mainly on the percentage of the LNCs without lecithin in the formulation. The mechanisms of formation and composition of interfacial layer containing intact LNCs and eventually triglyceride and FP molecules depend on the degree of surface saturation. Minkov et al. (2005) performed their experiments on the flat surface of a bulk liquid, and it must be mentioned that the size and the curvature of the surface of aqueous aerosol droplets could affect significantly the diffusion flux of LNCs towards the surface and the amount and composition of the spread material.

In contrast to the conventional microparticle suspensions for nebulization, the nanoparticles in aqueous colloidal dispersions can be more easily incorporated into the respirable fraction of aerosol droplets (Mc Callion et al., 1996). Using the nano-sized dispersion increases the probability that the drug distribution in the droplets is homogenous. Ostrander et al. (1999) demonstrated that 12.5 drug crystals of 200 nm in diameter would be contained in each 2 μm droplet and only 1.25 drug crystals of 2 μm would be contained in each 100 droplets. The mass median aerodynamic diameter of the nebulized LNC aqueous dispersion was 2.7 ± 0.1 μm (Hureaux et al., 2009), therefore the FP within 30–100 nm LNCs is likely to be homogenously distributed among the droplets.

The encapsulation efficiency after nebulization was the same as before nebulization, indicating that the FP remained associated with the LNCs during the nebulization process. Similarly, no change in the drug encapsulation in paclitaxel-loaded LNCs was observed after nebulization (Hureaux et al., 2009). In contrast, the disruption of liposomes and leakage of the encapsulated ciprofloxacin was observed (Finlay and Wong, 1998). In another study by Kleemann et al. (2007), leakage of iloprost was observed from nebulized liposomes (20–70% drug encapsulation post-nebulization), which was accompanied by a decrease in particle size. On the other hand, Hajos et al. (2008) did not observe the release of vasoactive intestinal peptide (VIP) from nebulized liposomes. The VIP molecules were efficiently associated with the liposomal formulation, exhibiting a strong negative surface charge, resulting in electrostatic interactions (Hajos et al., 2008). Therefore, the drug release from the nanocarriers during nebulization may depend on the partition of the drugs between the nanocarriers and the medium. If the drug is lipophilic or if strong interactions occur between the drug and the carrier, the drug remains associated with the carrier. On the other hand, if the drug is encapsulated inside the nanocarrier, as in the case of liposomes, disruption of the carrier structure may induce drug release.

Apart from particle characteristics, stability during nebulization and aerosol characteristics, other important factors such as the output rate should also be considered. Nebulized medications and excipients can change the aerosol output and the nebulization time due to changes in the physico-chemical properties of the solution or suspension, e.g., surface tension, viscosity, and density (Arzhavitina and Steckel, 2010). The study by Hureaux et al. (2009) showed that 3 ml of the 50 nm LNCs were nebulized by the eFlow nebulizer in less than 9 min. This study demonstrated that the nebulization time was not affected by either drug concentration or particle size (Table 5). The nebulization time and the output rate were mainly dependent on the LNC concentration. LNCs at 177 mg/ml were nebulized within 8–10 min, and 10-fold dilution decreased the nebulization time by approximately half.

Table 5
Nebulization time (in minutes) of LNC formulations nebulized at different concentrations. The nebulizer output can be calculated dividing the nebulization time by the amount of the formulation nebulized (2 ml).

LNC concentration	177 mg/ml	17.7 mg/ml	3.54 mg/ml
LNC30	9–10	4–5	3.5–4.5
LNC30FP250	9–10	4–5	-
LNC30FP500	9–10	4–5	
LNC30FP1000	9–10	4–5	-
LNC60	9–10	4–5	3.5–4.5
LNC60FP250	9–10	4–5	-
LNC60FP500	9–10	4–5	-
LNC60FP1000	9–10	4–5	-
LNC100	8–9	4–5	3.5–4.5
LNC100FP250	8–9	4–5	-
LNC100FP500	8–9	4–5	-
LNC100FP1000	8–9	4–5	-

4. Conclusions

FP was successfully loaded into LNCs, with the encapsulation efficiency found to depend on the quantity of FP added to the formulation and on the composition of the formulation, especially the quantity of the oil (C8/C10-TG). Small, homogenously dispersed nanocapsules were obtained, and the size could be conveniently modulated by modifying the composition of the sample. The information about the solubility of the drug in oil and water as well as the oil/water partition coefficient can be useful tools to assess the encapsulation of the drug in the LNC formulation.

Although the particle size and size distribution of nebulized LNCs were observed to increase significantly compared with control LNCs before nebulization, nebulization did not lead to the leakage of FP from the formulation. Additionally, despite the

increase in particle size, no phase separation was observed, and most nebulized LNCs were characterized by a small size below 150 nm. A small fraction of larger aggregates was responsible for the increase in the intensity-averaged particle diameter. LNC100 can be considered superior to LNC30 and LNC60, as these particles exhibit a better FP-loading capacity and better stability during nebulization.

Acknowledgements

This study was funded by Zcube (Italy). Author CRA Mouzouvi was funded by 'Service de Cooperation et d'Action Culturelle' of the French Embassy in Benin and by 'Ministère de l'Enseignement Superieur et de la Recherche Scientifique du Bénin'.

References

Arzhavitina, A., Steckel, H., 2010. Surface active drugs significantly alter the drug output rate from medical nebulizers. Int. J. Pharm. 384, 128–136.
Azarmi, S., Roa, W.H., Löbenberg, R., 2008. Targeted delivery of nanoparticles for the treatment of lung diseases. Adv. Drug Deliv. Rev. 60, 863–875.
Bailey, M.M., Berkland, C.J., 2009. Nanoparticle formulations in pulmonary drug delivery. Med. Res. Rev. 29, 196–212.
Beck-Broichsitter, M., Gauss, J., Packhaeuser, C.B., Lahnstein, K., Schmehl, T., Seeger, W., Kissel, T., Gessler, T., 2009. Pulmonary drug delivery with aerosolizable nanoparticles in an *ex vivo* lung model. Int. J. Pharm. 367, 169–217.
Binks, B.P., 2002. Particles as surfactants – similarities and differences. Curr. Opin. Colloid Interface Sci. 7, 21–41.
Borgström, L., 2001. The importance of the device in asthma therapy. Resp. Med. 95, S26–S29.
Bunjes, H., 2010. Lipid nanoparticles for the delivery of poorly water-soluble drugs. J. Pharm. Pharmacol. 62, 1637–1645.
Mc Callion, O.N.M., Taylor, K.M.G., Thomas, M., Taylor, A.J., 1996. Nebulisation of monodisperse latex sphere suspensions in air-jet and ultrasonic nebulisers. Int. J. Pharm. 133, 203–214.
Chiang, P.-C., Hu, Y., Thurston, A., Sommers, C.D., Guzova, J.A., Kahn, L.E., Lai, Y., Blom, J.D., 2009. Pharmacokinetic and pharmacodynamic evaluation of the suitability of using fluticasone and an acute rat lung inflammation model to differentiate lung versus systemic efficacy. J. Pharm. Sci. 98, 4354–4364.
Chiang, P.-C., Hu, Y., Blom, J., Thompson, D.C., 2010. Evaluating the suitability of using rat models for preclinical efficacy and side effects with inhaled corticosteroids aerosol suspension formulations. Nanoscale Res. Lett. 5, 1010–1019.
Cipolla, D., Shekunov, B., Blanchard, J., Hickey, A., 2014. Lipid-based carriers for pulmonary products: preclinical development and case studies in humans. Adv. Drug Deliv. Rev. 75, 53–80.
Dahl, R., 2006. Systemic side effects of inhaled corticosteroids in patients with asthma. Respir. Med. 100, 1307–1317.
Dailey, L.A., Schmehl, T., Gessler, T., Wittmar, M., Grimminger, F., Seeger, W., Kissel, T., 2003. Nebulization of biodegradable nanoparticles: impact of nebulizer technology and nanoparticle characteristics on aerosol features. J. Control. Release 86, 131–144.
Delmas, T., Fraichard, A., Bayle, P.-A., Texier, I., Bardet, M., Baudry, J., Bibette, J., Couffin, A.-C., 2012. Encapsulation and release behavior from lipid nanoparticles: model study with nile red fluorophore. J. Colloid Sci. Biotechnol. 1, 16–25.
Derendorf, H., Hochhaus, G., Meibohm, B., Möllmann, H., Barth, J., 1998. Pharmacokinetics and pharmacodynamics of inhaled corticosteroids. J. Allergy Clin. Immunol. 101, S446–S446.
Desai, T.R., Hancock, R.E.W., Finlay, W.H., 2002. A facile method of delivery of liposomes by nebulization. J. Control. Release 84, 69–78.
Doktorová, S., Araújo, J., Garcia, M.L., Rakovský, E., Souto, E.B., 2010. Formulating fluticasone-propionate in novel PEG containing nanostructured lipid carriers (PEG-NLC). Colloid Surf. B 75, 538–542.
Finlay, W.H., Wong, J.P., 1998. Regional lung deposition of nebulized liposome-encapsulated ciprofloxacin. Int. J. Pharm. 167, 121–127.
Hajos, F., Stark, B., Hensler, S., Prassl, R., Mosgoeller, W., 2008. Inhalable liposomal formulation for vasoactive intestinal peptide. Int. J. Pharm. 357, 286–294.
Heurtault, B., Saulnier, P., Pech, B., Proust, J.-E., Benoit, J.-P., 2002. A novel phase inversion based process for the preparation of lipid nanocarriers. Pharm. Res. 19, 875–880.
Heurtault, B., Saulnier, P., Pech, B., Benoit, J.P., Proust, J.E., 2003. Interfacial stability of lipid nanocapsules. Colloid Surf. B 30, 225–233.
Hirsjarvi, S., Bastiat, G., Saulnier, P., Benoit, J.-P., 2012. Evaluation of the wall deformability of lipid nanocapsules by drop tensiometer technique, and its experimental assessment by dialysis and tangential flow filtration. Int. J. Pharm. 434, 460–467.
Hureaux, J., Lagarce, F., Gagnadoux, F., Vecellio, L., Clavreul, A., Roger, E., Kempf, M., Racineux, J.-L., Diot, P., Benoit, J.-P., Urban, T., 2009. Lipid nanocapsules: ready-to-use nanovectors for the aerosol delivery of paclitaxel. Eur. J. Pharm. Biopharm. 73, 239–246.
Huynh, N.T., Passirani, C., Saulnier, P., Benoit, J.P., 2009. Lipid nanocapsules: a new platform for nanomedicine. Int. J. Pharm. 379, 201–209.
Kleemann, E., Schmehl, T., Gessler, T., Bakowsky, U., Kissel, T., Seeger, W., 2007. Iloprost-containing liposomes for aerosol application in pulmonary arterial hypertension: formulation aspects and stability. Pharm. Res. 24, 277–287.
Lamprecht, A., Bouligand, Y., Benoit, J.-P., 2002. New lipid nanocapsules exhibit sustained release properties for amiodarone. J. Control. Release 84, 59–68.
Lamprecht, A., Saumet, J.-L., Roux, J., Benoit, J.-P., 2004. Lipid nanocarriers as drug delivery system for ibuprofen in pain treatment. Int. J. Pharm. 278, 407–414.
Lamprecht, A., Benoit, J.-P., 2006. Etoposide nanocarriers suppress glioma cell growth by intracellular drug delivery and simultaneous P-glycoprotein inhibition. J. Control. Release 112, 208–213.
Malzert-Fréon, A., Saint-Lorant, G., Hennequin, D., Gauduchon, P., Poulain, L., Rault, S., 2010. Influence of the introduction of a solubility enhancer on the formulation of lipidic nanoparticles with improved drug loading rates. Eur. J. Pharm. Biopharm. 75, 117–127.
Manconi, M., Aparicio, J., Vila, A.O., Pendás, J., Figueruelo, J., Molina, F., 2003. Viscoelastic properties of concentrated dispersions in water of soy lecithin. Colloid Surf. A 222, 141–145.
Minkov, I., Ivanova, Tz., Panaiotov, I., Proust, J., Saulnier, P., 2005. Reorganization in lipid nanocapsules at air–water interface. I. Kinetics of surface film formation. Colloids Surf. B 45, 14–23.
Nirale, N.M., Vidhate, R.D., Nagarsenker, M.S., 2009. Fluticasone propionate liposomes for pulmonary delivery. Ind. J. Pharm. Sci. 71, 709–711.
Niven, R.W., Schreier, H., 1990. Nebulization of liposomes. I. Effect of lipid composition. Pharm. Res. 7, 1127–1133.
Niven, R.W., Speer, M., Schreier, H., 1991. Nebulization of liposomes. II. The effects of size and modeling of solute release profiles. Pharm. Res. 8, 217–221.
Ostrander, K.D., Bosch, H.W., Bondanza, D.M., 1999. An in-vitro assessment of a NanoCrystal™ beclomethasone dipropionate colloidal dispersion via ultrasonic nebulization. Eur. J. Pharm. Biopharm. 48, 207–215.
Sakagami, M., 2006. In vivo, in vitro and ex vivo models to assess pulmonary absorption and disposition of inhaled therapeutics for systemic delivery. Adv. Drug Deliv. Rev. 58, 1030–1060.
Sung, J.C., Pulliam, B.L., Edwards, D.A., 2007. Nanoparticles for drug delivery to the lungs. Trends Biotechnol. 25, 563–570.
Tsapis, N., Bennett, D., Jackson, B., Weitz, D.A., Edwards, D.A., 2002. Trojan particles: Large porous carriers of nanoparticles for drug delivery. Prot. Natl. Acad. Sci. U. S. A. 99, 12001–12005.
Umerska, A., Paluch, K.J., Santos-Martinez, M.J., Corrigan, O.I., Medina, C., Tajber, L., 2014a. Self-assembled hyaluronate/protamine polyelectrolyte complexes: synthesis, stability, biocompatibility, and potential use as peptide carrier. J. Biomed. Nanotechnol. 10, 3658–3673.
Umerska, A., Corrigan, O.I., Tajber, L., 2014b. Intermolecular interactions between salmon calcitonin, hyaluronate, and chitosan and their impact on the process formation and properties of peptide-loaded nanoparticles. Int. J. Pharm. 437, 102–112.
Umerska, A., Paluch, K.J., Santos-Martinez, M.J., Medina, C., Corrigan, O.I., Tajber, L., 2015. Chondroitin-based nanoplexes as peptide delivery systems – investigations into the self-assembly process, solid-state and extended release characteristics. Eur. J. Pharm. Biopharm. 93, 242–253.
Weber, S., Zimmer, A., Pardeike, J., 2014. Solid lipid nanoparticles (SLN) and nanostructured lipid carriers (NLC) for pulmonary application: a review of the state of the art. Eur. J. Pharm. Biopharm. 86, 7–22.
Yang, J.Z., Young, A.L., Chiang, P.-C., Thurston, A., Pretzer, D., 2008. Fluticasone and budesonide nanosuspensions for pulmonary delivery: preparation, characterization, and pharmacokinetic studies. Eur. J. Pharm. Sci. 97, 4860–4878.